Proceedings of International Conference on Heat Exchanger Fouling and Cleaning - 2011 (Peer-reviewed)
June 05 - 10, 2011, Crete Island, Greece
Editors: M.R. Malayeri, H. Müller-Steinhagen and A.P. Watkinson

Published online
www.heatexchanger-fouling.com

FOULING OF EGR HEAT EXCHANGERS – INVESTIGATION OF MECHANISMS INVOLVED IN SOOT PARTICLE DEPOSITION

G. Hörnig[1], P. Völk[2], G. Wachtmeister[2] and R. Niessner[1]

[1]Technische Universität München, Institute of Hydrochemistry, Chair for Analytical Chemistry,
Marchioninistr. 17, D – 81377 Munich, Germany, e-mail: gabriele.hoernig@ch.tum.de
[2]Technische Universität München, Institute of Combustion Engines, Schragenhofstr. 31, D – 80992 Munich, Germany

ABSTRACT

Cooled exhaust gas recirculation (EGR) is a very effective method to reduce nitrogen oxide emissions of diesel engines. However, due to particulate matter and other components present in diesel exhaust gas, EGR coolers are highly prone to fouling.

As different soot deposition mechanisms are acting inside the coolers, various model cooler experiments were performed to clarify their contribution to cooler fouling.

A model aerosol was used, containing soot particles either with or without hydrocarbon (HC), water and sulphuric acid (H_2SO_4) vapour added.

The additive-free soot aerosol became deposited due to thermal forces under corresponding temperature conditions. Turbulent eddy diffusion increased size-dependent deposition efficiencies especially for particles smaller than 50 nm.

However, the aerosol containing water, HC and H_2SO_4 vapour showed an even higher potential for deposit build-up. Thus we found that condensation and diffusiophoresis contribute essentially to EGR cooler fouling, as diesel exhaust always contains condensable components.

INTRODUCTION

The combustion process in diesel engines is a source for hazardous environmental pollutants such as nitrogen oxides (NO_x) or particulate matter (soot). Future emission standards (e.g. Regulation (EC) N^O 715/2007 of the European Parliament and of the Council, 2007) require increased application of exhaust gas recirculation (EGR). EGR is a very simple though effective way to reduce NO_x emissions in diesel exhaust. A fraction of the emitted flue gas is cooled in an EGR cooler, returned to the engine and mixed with fresh charge air. Due to the decreased oxygen content, NO_x emission is eventually reduced (Ladommatos et al., 2000).

Besides the usual combustion end products the recycled exhaust gas also contains unburnt hydrocarbons (HC), soot particles, metal oxides and traces of sulphuric acid (H_2SO_4) (Kittelson, 1998). These constituents are responsible for EGR coolers being very prone to fouling during vehicle lifetime. Due to various acting deposition mechanisms an insulating layer forms on the gas side of the EGR cooler which reduces heat transfer and thus the cooling efficiency of the device. As an additional consequence pressure losses are increased (Abd-Alla, 2002). Therefore, today's EGR coolers are designed to meet the limitations for NO_x output despite the efficiency decrease. In general, this means that EGR coolers are oversized to compensate the rate of fouling by cooling efficiency reserves.

Deposition mechanisms

The most important deposition mechanisms acting in EGR coolers are in alphabetical order:

- *Diffusion*, where small particles are transported to the cooler wall due to undirected Brownian particle motion. The effect of diffusion is strongly dependent on particle size, flow velocity and cooler geometry (Friedlander, 2000; Gormley and Kennedy, 1949).

- *Diffusiophoresis*, where the condensation of one or several gaseous components causes a vapour concentration gradient, inducing directed particle transport towards the surface on which condensation is happening. This effect depends on the condensate mass flow defined by the strength of the vapour concentration gradient as well as on the gas and particle velocities (Hirschfelder, 1954). It is known that diffusiophoresis may occur in exhaust gas cooler applications and enhance particle deposition. Lehtinen et al. (2002) and Gröhn et al. (2009) for example studied the effect of condensation on particle deposition. However, these authors only took the condensation of water vapour into account, whereas diesel exhaust gas also contains condensable diesel fuel components and sulphuric acid.

- *Impaction*, where inertia causes particles larger than a critical size to deposit in case of redirection of the gas flow. The critical particle size is strongly dependent on cooler geometry and gas flow velocity (Hinds, 1999).

- *Thermophoresis*, where a temperature gradient leads to transport of particles from the hot gas to the cold wall. For this mechanism temperature, flow conditions and cooler geometry are important (Messerer et al., 2003, Romay et al., 1998). This mechanism is often described as being the most important acting mechanisms in heat exchanger fouling (e.g. Abarham et al., 2010).

The aim of this work is to gain more understanding of the mechanisms leading to the build-up of an insulating layer and all parameters influencing these mechanisms.

Some precise concepts about the principles already exist, however the individual influencing variables and their significance for the deposit formation inside EGR coolers needed to be worked out in detail.

Extensive experimental series were conducted to analyze the influence of parameter variations on the deposit build-up. One set of experiments was conducted to determine the parameters leading to an increased mass-based deposition efficiency of a polydisperse soot aerosol. A second set of experiments determining the size-dependent deposition efficiency was performed to gain insight into particle size effects and spatial particle deposition.

EXPERIMENTAL

Setup

Different diesel exhaust gas compositions are simulated on a test bench using a custom-built tube-in-tube air-to-water heat exchanger and model aerosols. The test bench setup is shown in Figure 1. The cooler setup with the exchangeable inner tube is depicted in Figure 2. This inner tube is made of aluminium with a length of 160 mm, an outer diameter of 12 mm and a wall thickness of 1 mm. It can be easily removed for further measurements and cleaning.

The smoothly curved cooler entrance resulted from previously performed tests on real EGR coolers. These tests showed that suddenly changing entrance geometries are very prone to fouling caused by impaction and interception of soot particles. As a result the heat exchanger tubes get blocked before hot gas can pass the cooling section (Hörnig et al., 2010). Since our focus is on the processes happening inside the cooled section of the heat exchanger, this layout was chosen to avoid blocking of the tubes.

The cooling circuit consists of a thermostat (Haake K20/DC1, Thermo Haake GmbH) connected to the model cooler, where a 3:2 water – antifreeze (Glysantin®, BASF) mixture is brought to and maintained on the desired coolant temperature. The coolant mass flow is kept constant at 4 L min^{-1}, cooling the heat exchanger in counter flow.

Temperatures are determined using K-Type thermocouples installed at the cooler inlet and outlet (positions shown in Figure 2) as well as in the coolant feed (HKMTSS-IM150U-150, Omega Engineering, Inc.).

Pressure before and after the cooler are determined using two CTE 7000 miniature pressure transmitters (SensorTechnics, positions shown in Figure 2).

Particle size distributions are determined using a scanning mobility particle sizer (SMPS, TSI). Therefore a fraction of the aerosol was taken out of the system using a probing tip. The tip's form and its positioning are in accordance with Directive 1999/96/EG of the European Parliament and of the Council, 1999.

Model aerosol production

Real diesel exhaust is simulated by generating a model soot aerosol. The model aerosol is produced by first heating dry particulate free pressurized air to the desired temperature. This task is performed by leading the gas feed line through an oven (Carbolite 1200 °C, Barloworld Scientific).

The gas temperature then is kept constant along the feed line until the gas enters the cooler by using tube jacket heating (heating tapes HSQ, Hillesheim AG, controller HT 40, Hillesheim AG). Gas temperatures of up to 450 °C are thus achievable. The gas mass flow passing through the system is continuously adjustable by a mass flow meter (red-y smart meter GSM, Vögtlin Instruments AG). Thus variation of flow velocities is possible, typical Reynolds numbers are in the range 5,000 < Re < 10,000.

Before entering the cooler, soot either produced by the flame of a diffusion burner (following CAST principle; Jing, 2000) or by a spark discharge generator (GfG 1000, Palas GmbH) is added to the hot air stream, depending on the type of experiment.

Particle sizes between 10 nm and 600 nm with a size distribution equal to soot emitted from a turbocharged diesel engine (M57D30 TÜ2, BMW) (d_{median} = 120 ± 5 nm, σ_g = 1.77) can thus be provided. The particle number concentrations are in the range of 10^5 to 10^7 particles per cubic centimetre which is slightly lower than that determined for real diesel exhaust gas where number concentrations are in the range of 10^{10} particles per cubic centimetre, depending on operating conditions of the engine.

Water, sulphuric acid and diesel fuel are added to the aerosol in different concentrations which are comparable to those present in real diesel engine exhaust gas to study their effect on deposit build-up. The particle size distribution does not change due to the addition of vapour components. This is made sure by control SMPS measurements.

The water content of diesel exhaust gas is usually in the range of 2 % (w/w) to 8 % (w/w) (Dietsche, 2007). Due to a drop in gas temperature when vaporizing water in the test system (enthalpy of evaporation) only a maximum water vapour concentration of 5 % (w/w) is viable at the model test bench.

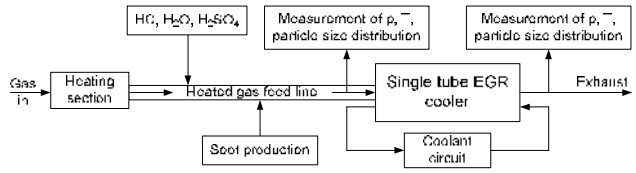

Fig. 1 Schematic setup of model test bench.

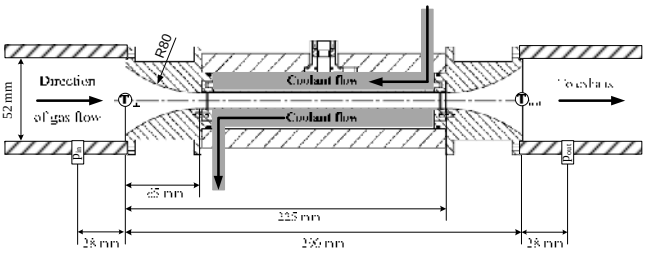

Fig. 2 Cross-sectional view of the model cooler. Positions of thermocouples used for measuring gas in- and outlet temperatures and of pressure sensors are shown.

HC concentrations are chosen on the basis of measurements performed at the engine test bench of the Institute of Combustion Engines (TU Munich), where the total HC content in the exhaust gas is relatively high with 200 ppm to 450 ppm. These high concentrations are due to operating the engine with late post-injection. This procedure is chosen to achieve a faster deposit formation in the regarded model cooler (Hörnig et al., 2011). Very high HC concentrations (1200 ppm) are chosen to simulate a peak value in order to demonstrate the influence of high HC concentrations on deposition build-up more clearly. To comply with the requirement of generating a model aerosol as similar to real diesel exhaust gas as possible, the same commercially available diesel fuel (B7 according to DIN EN 590) that was used for the engine test bench was injected into the hot gas.

The amount of sulphuric acid in the exhaust gas is dependent on the sulphur content of the used fuel. Due to legal requirements (DIN EN 590) today's diesel fuels for passenger cars and light duty vehicles have sulphur content of less than 10 ppm. This sulphur can be converted to sulphuric acid via SO_3 production, resulting in sulphuric acid aerosol in the exhaust gas of less than 0.1 ppm. Yet in our experiments we use higher concentrations of sulphuric acid (0.2 ppm, 0.5 ppm and 10 ppm). On the one hand this helps us to gain more information on the effect of diffusiophoresis. On the other hand, heavy duty engines still use fuel with sulphur content of up to 1000 ppm. Manufacturers of EGR applications for these engines report on great problems with acid condensation (private communication with industry partners).

Determination of mass-based deposition efficiency

The deposition experiments are performed using polydisperse soot aerosol from the diffusion burner with different additives. This source of soot is used because it provides a sufficiently high and constant mass flow ($\dot{m}_{soot,in}$ = 45 mg h^{-1}) of soot that in its composition is comparable to diesel engine soot (Jing, 2000).

Gas and coolant temperatures and thus the temperature differences within the cooler are varied. For all experiments the largest temperature difference is determined as difference between gas inlet temperature and coolant temperature:

$$\Delta T_{max} = T_{gas} - T_C \qquad (1)$$

In Table 1 all conditions regarded are listed. Gas mass flow for all experiments is $\dot{m}_{gas}$ = 5.5 kg h^{-1} and system pressure is kept at ambient pressure.

Deposited mass is determined by weighing the cooler tubes before and after an experimental time of three hours under similar conditions. Particle inlet mass flow is determined by collecting particles on filters or is calculated from the size distribution, which is continuously determined using SMPS. The mass-based deposition efficiency ε_m of the model cooler is calculated as:

$$\varepsilon_m = \frac{m_{soot,deposited}}{\dot{m}_{soot,in} \cdot t} \cdot 100\% \qquad (2)$$

Table 1: Conditions for deposition experiments and results for mass-based deposition efficiencies (calculated from Eq. (2)). Gas mass flow for all experiments: $\dot{m}_{gas}$ = 5.5 kg h^{-1}; duration of all experiments: 3 h; polydisperse flame soot ($\dot{m}_{soot,in}$ = 45 mg h^{-1}).

	H_2O [% w/w]	HC [ppm]	H_2SO_4 [ppm]	T_{gas} [°C]	T_C [°C]	ΔT_{max} [°C]	**ε_m [%]**	Number of experiments
Dry soot				160	80	80	**7**	1
				300	20	280	**14 ± 10**	3
Soot + H_2O	1			300	20	280	**11**	1
	2			400	20	380	**14 ± 7**	3
	5			400	20	380	**11 ± 2**	3
Soot + HC		230		400	20	380	**18 ± 13**	3
		430		400	20	380	**21 ± 2**	3
Soot + H_2O + HC	1	230		155	20	135	**33**	1
	2	430		190	20	170	**49**	1
	2	430		400	20	380	**18 ± 3**	3
	2	430		400	80	320	**16**	1
Soot + H_2O + HC + H_2SO_4	2	430	0.2	150	20	130	**42 ± 13**	3
	2	430	0.2	150	80	70	**22 ± 5**	3
	2	430	10	150	20	130	**88 ± 15**	3
	2	430	10	400	20	380	**58 ± 43**	3
	5	1200	0.2	150	20	130	**15 ± 9**	3

Determination of size-dependent deposition efficiency

The size-dependent deposition efficiency is determined using dry monodisperse spark discharge soot aerosol. In combination with a Differential Mobility Analyzer (DMA, Model 3071, TSI) the GfG soot generator allowed production of stable monodisperse aerosols with particle sizes between 10 nm and 200 nm. The particle concentrations of the monodisperse model aerosol are determined at different positions within the cooler using a Faraday Cup Electrometer (FCE). Number concentrations of the monodisperse aerosols are in the range of 10^3 to 10^5 particles per cubic centimetre, depending on the selected particle size.

Soot concentration is not adjusted to be constant, when gas mass flow is varied. However, for the determination of the size dependent deposition efficiency, the entrance soot concentration is constantly monitored.

Gas and coolant temperatures and thus the temperature differences within the cooler again are varied. To isolate effects not caused by thermal forces, isothermal experiments are performed at $T_C = T_{gas} = 20$ °C. The parameters, including selected particle sizes, are listed in Table 2.

The space-resolved measurements are performed using a specially designed sampling probe ($d_i = 1.5$ mm, L = 1 m), which can be moved through the cooler along its central axis. The setup is shown in Figure 3. Due to the changed setup, system pressure and outlet temperature data were not collected for these experiments.

For all measurements the particle concentration is determined in the following way: after ensuring the system is set to the desired temperature and mass flow conditions, the first monodisperse aerosol was injected. The concentration was recorded for five minutes at x = 0 mm in order to obtain a reference concentration N(x = 0). Then position of the sampling probe was changed and the concentration at the new position x was recorded again for 5 minutes. After the last x position, the sampling probe was moved back to x = 0, before the next particle size was regarded. Depending on the number of x positions and particle sizes regarded, experimental time thus varied between 90 minutes and 7.5 hours. To ensure that time effects could be ruled out, measurements were repeated, using the different monodisperse aerosols in different order.

Thus it is possible to determine the fraction of particles deposited within the cooler using the following equation.

$$\varepsilon_n = \frac{N(x=0) - N(x)}{N(x=0)} \cdot 100\,\% = \left(1 - \frac{N(x)}{N(x=0)}\right) \cdot 100\,\% \qquad (3)$$

Table 2: Parameters varied for determination of size-dependent deposition efficiency.

Parameter	Regarded settings
T_{gas} [°C]	150, 300
T_C [°C]	20, 40, 60, 80
$\dot{m}_{gas}$ [kg h^{-1}]	5,10, 15
d_p [nm]	11, 16, 22, 26, 31, 36, 52, 70, 76, 95, 113, 123, 144, 159, 173, 186, 199

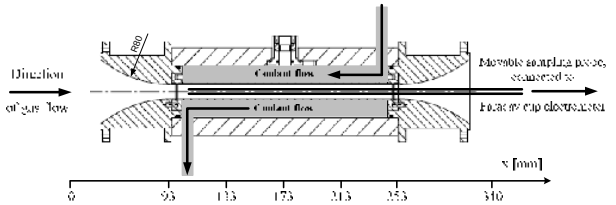

Fig. 3 Setup for space-resolved particle measurements, showing placement of sampling probe and measurement positions.

RESULTS AND DISCUSSION

Mass-based deposition efficiency

We observed that a test time of 3 h was long enough to create a perceptible deposit layer within the model heat exchanger (data not shown). However, the structure of the deposit layer was strongly dependent on aerosol composition and experimental conditions. There was no significant change in pressure drop detected during our experiments.

Dry soot deposition. When the aerosol consisted only of dry air and soot particles, ε_m was small due to thermal forces but increased with increasing temperature gradients established inside the cooler. For a temperature difference of $\Delta T_{max} = 80$ °C deposition efficiency was $\varepsilon_m = 7$ %. When ΔT_{max} was raised to 280 °C the deposition efficiency increased to $\varepsilon_m = 14$ %. The deposited particles were evenly distributed over the length of the tube. However, further increase of ΔT_{max} did not increase ε_m.

Water condensation. For experiments with a water vapour concentration of 1 % (w/w) and 2 % (w/w), the deposited particles were evenly distributed over the tube length. For water content of 5 % (w/w) a wash out effect was observed where blank metal was visible near the outlet of the cooler. The value for ε_m in all cases was between 11 % and 14 %, which was comparable to that of dry soot.

However, only the mass-based deposition efficiency was determined in these experiments. Particulate mass might have been washed out of the cooler due to condensation effects and thus is not accounted for by the gravimetric analysis. A deposition enhancing effect of water vapour condensation can not be ruled out at this point of our research because in the experiments where HC and H_2SO_4 were available for condensation, the mass-based deposition efficiency significantly increased.

HC and H_2SO_4 condensation. A HC concentration of 230 ppm at high gas and low coolant temperature resulted in $\varepsilon_m = 18$ %, which was slightly larger compared to the dry soot only and soot with water conditions. Increasing the HC concentration to 430 ppm led to a deposition efficiency of 21 %. Deposition build-up thus increased with increasing HC content of the gas.

When HC and water vapour were simultaneously added to the soot particles, ε_m was comparable to that of HC only addition (ε_m = 18%) under the same temperature conditions (T_{gas} = 400 °C, T_C = 20 °C). When under identical conditions the coolant temperature was raised to 80 °C, deposition efficiency did not significantly decrease (ε_m = 16 %). Lower gas (190 °C) and coolant (20 °C) temperatures had a more distinct effect on ε_m. Here its value increased to 49 % as the low gas temperature favoured condensation and particles became deposited due to the combined effects of thermo- and diffusiophoresis. However, at the same time the amount of condensate was too small to cause wash out effects.

For lower water vapour and HC concentrations (1 % (w/w) and 230 ppm, respectively), a gas temperature of 155 °C and a coolant temperature of 20°C we still found ε_m = 33 % as condensation increased with decreasing gas and wall temperatures.

When adding water, HC and H_2SO_4 (2 % (w/w), 430 ppm and 0.2 ppm, respectively), wall temperature showed a larger effect on deposit formation at low gas temperature (150 °C). For T_C = 20 °C ε_m was 42 %, for T_C = 80 °C ε_m dropped to 22 %. Again condensation effects were observed and deposition was considerably larger than for dry soot.

When the acid concentration was kept low and water and HC concentrations were increased, ε_m decreased to 15 %. Yet, for these measurements wash out effects which might be responsible for the drop of efficiency could not be accounted for.

When increasing the H_2SO_4 concentration to 10 ppm and keeping water and HC contents also on a high level, ε_m went up to 58 % for T_{gas} = 400 °C and even up to 88 % for T_{gas} = 150 °C, again showing that at low gas temperatures condensation effects enhance deposit formation.

Thus we see that for heavy-duty diesel applications, where sulphur contents in the fuel are higher than in those for light-duty vehicles, acid condensation significantly contributes to particle deposition in the corresponding EGR applications.

Data variability. The mass-based deposition efficiencies determined in the deposition measurements showed rather large deviations for certain experimental conditions. These mass-based deposition efficiencies were determined experimentally from the mass of deposit inside the cooler tube using equation 2. However, it is possible that e.g. through condensation of water vapour parts of the deposits are washed out from the cooler. Thus a fraction of the deposit is not accounted for by gravimetric analysis. Due to time limitations only three replicates of the most relevant conditions were examined. However, variations of ± 15 % are in the usual range of gravimetric measurements. Only for one condition ε_m was found to be 58 ± 43 %, showing a much higher data variation. The three values for ε_m determined at this condition were 38%, 29% and 108%, respectively.

The last value surely is an outlier maybe caused by an undetected variation in aerosol production. But even if this data point is neglected, the overall trend of H_2SO_4 condensation enhancing deposit formation still remains.

Size-dependent deposition efficiency

Variation of coolant temperature. Figure 4 shows the size-dependent deposition efficiencies for a gas mass flow of $\dot{m}_{gas}$ = 5 kg h^{-1} and for different T_C determined at x = 340 mm (end of EGR cooler).

Increase of coolant temperature at constant T_{gas} = 300 °C decreased the maximum temperature difference ΔT_{max}. This led to a decrease in average particle deposition efficiency from ε_n (T_C = 20 °C) = 44% to ε_n (T_C = 80 °C) = 37%, due to a decline of the thermophoretic force. For T_C = 40 °C, 60 °C and 80 °C respectively, ε_n was found to be independent of particle size. Only for particles with diameters larger than 150 nm an increase of deposition efficiency was observed. For T_C = 20 °C, however, ε_n was found to also be larger for particles with 10 nm < d_P < 50 nm.

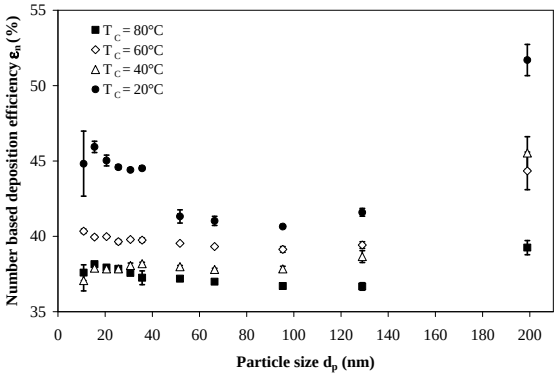

Fig 4 Particle deposition as a function of particle size and coolant temperature. $\dot{m}_{gas}$ = 5 kg h^{-1}, T_{gas} = 300 °C, T_C varied, x = 340 mm.

Influence of gas mass flow. Figure 5 shows ε_n for isothermal conditions (ΔT_{max} = 0 °C) and compares them with temperature gradient conditions (ΔT_{max} = 280 °C) for three different gas mass flows (5 kg h^{-1}, 10 kg h^{-1}, 15 kg h^{-1}). The data for this figure were also obtained measuring at position x = 340 mm.

For isothermal conditions and a gas mass flow of 1 kg h^{-1}, deposition ε_n was 0 % (data not shown). Increasing the gas mass flow to 15 kg h^{-1} under otherwise identical conditions, ε_n significantly increased to 25 %. With the temperature gradient present in the system, deposition efficiency further increased (ε_n = 40 %).

Again enhanced deposition of particles larger than 150 nm was observed. Additionally, ε_n were larger for particles smaller than 30 nm when gas mass flow was 10 kg h^{-1} and 15 kg h^{-1} respectively. Yet, under the given conditions deposition of small particles due to Brownian diffusion can be neglected. For diffusion, the deposition

efficiency ε_{diff} is determined according to the equation of Gormley and Kennedy (1949). Particles in the size range between 10 nm and 1000 nm have a deposition efficiency ε_{diff} smaller than 0.2 %.

Also, increase of gas mass flow leads to a dilution of the particle concentration, thus preventing agglomeration of the small soot particles inside the cooler (Friedlander, 2000).

It is thus assumed that turbulent eddy diffusion (Friedlander, 2000, Tsai et al., 2004) has a strong influence on transporting these small particles towards the cooler wall.

Since with tightened emission legislation the size of particles emitted by diesel engines is decreasing, an elevated deposition for these small particles significantly contributes to deposit formation in EGR applications.

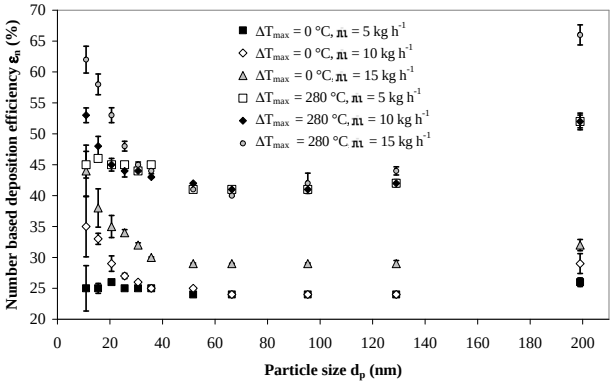

Fig. 5 Particle deposition as a function of particle size, temperature difference and gas mass flow. $\dot{m}_{gas}$ = 5, 10, 15 kg h^{-1}, ΔT_{max} = 0 °C and 280 °C, x = 340 mm.

Space-resolved measurements. Figure 6 shows ε_n of particles with a diameter of d_p = 26 nm for both isothermal conditions and at ΔT_{max} = 280 °C (T_{gas} = 300 °C, T_C = 20 °C). ε_n was determined for five different x-positions within the cooler tube, which were spaced with 40 mm distance, beginning at x = 93 mm. That the temperature effect (thermophoresis) increases particle deposition again is clearly visible.

This space-resolved measurement showed that ε_n did not change significantly over the length of the cooled section. However, particles deposited on the cooler wall were found. The measurements were performed in the centre of the air flow and only with dry soot.

This effect was true for all particles in the size range regarded (10 nm to 200 nm), independent of gas mass flow. The curves for all other particle sizes regarded looked similar (data not shown).

The previous experiments showed even smaller mass-based deposition efficiencies for the same conditions. However, if particle numbers are large enough, even effects leading to very small deposition efficiencies can cause significant deposit formation.

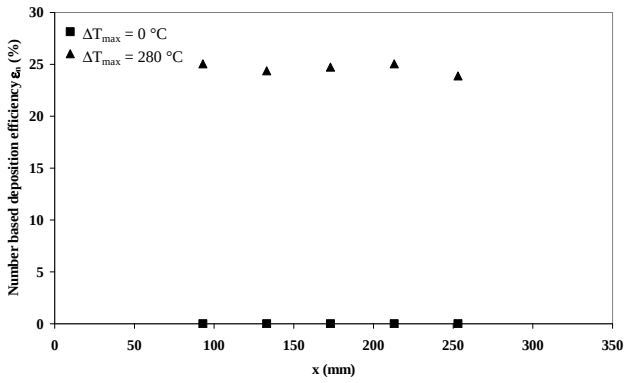

Fig. 6 Deposition efficiency versus cooler tube length (x varied), T_{gas} = 300 °C, T_C = 20 °C, d_p = 26 nm, $\dot{m}_{gas}$ = 5 kg h^{-1}.

CONCLUSIONS

1. Mass-based deposition efficiency:
   Conditions favouring condensation of vapour components, i.e. low coolant and gas temperatures, enable diffusiophoresis to act. This results in high mass-based deposition efficiencies showing that diffusiophoresis has a major contribution to EGR cooler fouling and needs to be considered besides thermophoresis.

2. Size-dependent deposition efficiency:
   Turbulent eddy diffusion and temperature effects increase deposition efficiencies especially for particles smaller than 50 nm. Effects inside the cooled section of the cooler are negligible.

3. The different mechanisms that are involved in the soot deposition within heat exchangers add to the formation of a soot layer. All of the mechanisms considered act most effective at the cooler inlet where geometry and temperature conditions are most favourable.

4. To improve EGR cooler performance, wash out effects due to water condensation should be specifically induced and conditions under which no water, but large amounts of hydrocarbons condense, should strictly be avoided.

5. Further experiments with different aerosol composition are still needed to describe the processes happening in the EGR coolers in greater detail.

ACKNOWLEDGEMENTS

This work was financially supported by Forschungsvereinigung Verbrennungskraftmaschinen (FVV e.V., Project N° 966 & N° 1048). Support by Sebastian Wiesemann from our mechanical workshop is gratefully acknowledged.

NOMENCLATURE

d_i	inner diameter, mm
d_p	particle size, nm
L	length, m
m	mass, kg
$\dot{m}_{gas}$	gas mass flow, kg h^{-1}
$\dot{m}_{soot,in}$	soot mass flow, mg h^{-1}
N	particle number concentration, m^{-3}
Re	Reynolds number, ρ u d_i/μ, dimensionless
T	temperature, °C
t	time, s
u	gas velocity, m/s
x	position, mm
ε_m	mass-based deposition efficiency, $m_{deposit}/(\dot{m}_{in}\, t)$, dimensionless
ε_n	size-dependent deposition efficiency, 1-N(x)/N(x = 0), dimensionless
ΔT	temperature difference, $T_{gas} - T_C$, °C
ρ	density, kg m^{-3}
μ	dynamic viscosity, kg/s m

Subscript

C coolant
diff diffusion
p particle

REFERENCES

Abarham, M., Hoard, J.W., Assanis, D., Styles, D., Sluder, C.S. and Storey, J.M.E., 2010, An analytical study of thermophoretic particulate deposition in turbulent pipe flows, *Aerosol Sci. Technol.*, Vol. 44, pp. 785-795.

Abd-Alla, G. H., 2002, Using exhaust gas recirculation in internal combustion engines: a review, *Energy Conversion & Management*, Vol. 43, pp. 1027-1042.

Dietsche, K.H., 2007, *Kraftfahrttechnisches Taschenbuch*, Vieweg & Sohn Verlag, Wiesbaden.

Friedlander, S.K., 2000, *Smoke, dust, and haze. Fundamentals of aerosol dynamics*, Oxford University Press, New York.

Gormley, P. and Kennedy, M., 1949, Diffusion from a stream flowing through a cylindrical tube, *Proceedings of the Royal Irish Academy*, Vol. 52A, pp. 163-169.

Gröhn, A., Suonmaa, V., Auvinen, A., Lehtinen, K.E.J. and Jokiniemi, J., 2009, Reduction of fine particle emissions from wood combustion with optimized condensing heat exchangers, *Environ. Sci. Technol.*, Vol. 43(16), pp. 6269-6274.

Hinds, W.C., 1999, *Aerosol technology. Properties, behavior, and measurement of airborne particles*, Wiley Interscience, New York.

Hirschfelder, J.O., 1954, *Molecular theory of gases and liquids*, John Wiley & Sons, New York.

Hörnig G., Völk, P., Niessner, R. and Wachtmeister, G., 2011, Verschmutzung von AGR-Kühlern I, Untersuchung der Ablagerungsmechanismen auf der gasseitigen Oberfläche von Abgaswärmeaustauschern und die Entwicklung von Lösungsansätzen zu ihrer Vermeidung und zum Ablösen der Ablagerung, Abschlussbericht, Heft 929, Forschungsvereinigung Verbrennungskraftmaschinen (FVV e.V) (in German).

Jing, L., 2000, Neuer Rußgenerator für Verbrennungs-teilchen zur Kalibrierung von Partikelmessgeräten, *OfmetInfo*, Vol. 7(2), pp. 1-5.

Kittelson, D., 1998, Engines and nanoparticles: a review, *J. Aerosol Sci.*, Vol. 29, pp. 575-588.

Ladommatos, N., Abdelhalim, S. and Zhao, H., 2000, The effects of exhaust gas recirculation on diesel combustion and emissions, *Int. J. Engine Research*, Vol. 1(1), pp. 107-126.

Lehtinen, K. E. J., Hokkinen, J., Jokiniemi, A.A.J.K. and Gamble, R.E., 2002, Studies on steam condensation and particle diffusiophoresis in a heat exchanger tube, *Nuclear Engineering and Design*, Vol. 213, pp. 67-77.

Messerer, A., Pöschl, U. and Niessner, R., 2003, Thermophoretic deposition of soot aerosol particles under experimental conditions relevant for modern diesel engine exhaust gas systems *J. Aerosol Sci.*, Vol. 34, pp. 1009-1021.

Romay, F., Takagaki, S., Pui D. and Liu, B., 1998, Thermophoretic Deposition of aerosol particles in turbulent pipe flow, *J. Aerosol Sci.*, Vol. 29, pp. 943-959.

Tsai, C., Lin, J.-S., Aggarwal, S. and Chen, D.-R., 2004, Thermophoretic deposition of particles in laminar and turbulent tube flows, *Aerosol Sci. Technol.*, Vol. 38, pp.131-139.